# Development of Middle Ear Acoustic Sensor for Fully Implantable Cochlear Prosthesis

Mark A. Zurcher, Darrin J. Young, and Wen H. Ko
Department of Electrical Engineering and Computer Science
Case Western Reserve University
Cleveland, OH, USA
Email: mark.zurcher@case.edu

Tung Trang, Maroun Semaan, and Cliff A. Megerian
Department of Otolaryngology – Head and Neck Surgery
University Hospitals of Cleveland
Cleveland, OH, USA

*Abstract*— **The current trend in cochlear implant technology is system miniaturization and steady progress towards a totally implantable prosthetic system. To achieve this objective the external microphone of present implants needs to be implantable. A miniature accelerometer placed on the ossicular chain in the middle ear can accomplish the objective by detecting and converting bone vibrations in response to incident sounds into an electrical signal for further processing and stimulating cochlear implant electrodes. This paper describes the optical characterization of human temporal bones for optimum sensor placement and reports the results of attaching a commercial accelerometer on the umbo for sound detection. The vibration acceleration frequency response in the direction perpendicular to the tympanic membrane increases with a slope of 40 dB per decade below 1 kHz and with a slope of about 20 dB per decade from 1 kHz to 4 kHz. Above 4 kHz the acceleration signal remains relatively flat. Throughout the measurement frequency range the vibration acceleration exhibits a linear function of the input sound pressure level (SPL) with a slope of 20 dB per decade. A commercial accelerometer is able to detect pure tone inputs with a minimum detectable signal of approximately 80 dB SPL at 500 Hz and 55 dB SPL at 2.4 kHz, which is the sensor bandwidth. An accelerometer with reduced package mass and improved performance, achieving a sensitivity of 50 $\mu g/\sqrt{Hz}$ and bandwidth of 10 kHz, would be needed to satisfy the requirements for normal conversation detection.**

***Keywords****- Acceleration measurement, Implantable biomedical devices, Laser vibrometry, Sound detection*

## I. INTRODUCTION

Sensorineural hearing loss affects over 20 million people in the United States. Although moderate rehabilitation in a large number of sensorineural hearing loss cases can be achieved with contemporary acoustic hearing aids, inherent technological limitations and perceived social stigma associated with these devices have resulted in many patients being deprived of basic hearing abilities. While partially implantable middle ear and cochlear prosthetic systems have gained acceptance, the use of external accessories such as microphones and electronics presents reliability, practicality, and social stigma concerns. It is, therefore, highly desirable to develop totally implantable high-performance prosthetic systems.

Progress has been made by several research groups [1]–[4] in developing prosthetic systems that rely on electromagnetic or piezoelectric effects for compensating conductive hearing loss, and external microphone, radio frequency coils, and speech processor for cochlear implants. However, to date no fully implantable prosthetic system is commercially available. To achieve complete implantability, current speech processors can be potentially integrated as a part of the existing implant unit. However, realizing a high performance implantable microphone presents a significant challenge. In this research a MEMS accelerometer is proposed as an implantable microphone for a future totally implantable cochlear prosthetic system. The conceptual prosthetic system architecture is shown in Fig. 1. The proposed middle ear sound sensor, based on accelerometer operating principle, can be attached to the umbo to convert the umbo vibration to an electrical signal representing the input acoustic information. This electrical signal can be further processed by the cochlear implant speech processor, which is followed by a stimulator to drive cochlear electrodes. The speech processor, stimulator, power management and control unit, rechargeable battery and radio-frequency (RF) coil will be housed in a biocompatible package located under the skin to form a wireless network with external adaptive control and battery charging system.

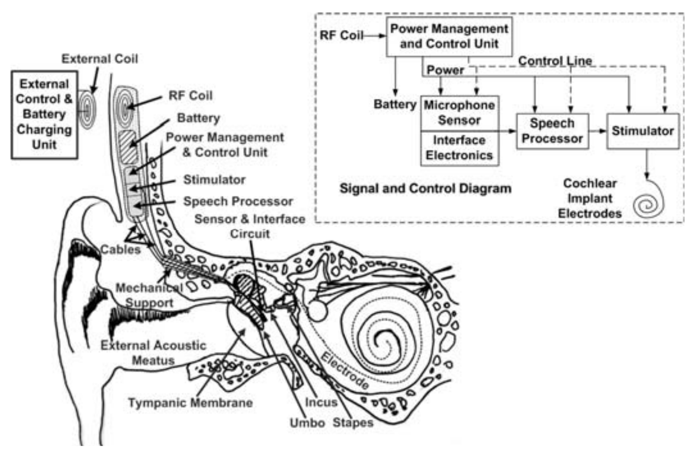


Fig. 1. Architecture of proposed fully implantable cochlear prosthetic system.

Wireless communication between the implant and external system is essential for post-implant programming of the speech processor. In practice, it is difficult to achieve precise

This work was supported by the National Institutes of Health under grant number: 5R21-DC-006850.

positioning and insertion control of cochlear electrodes during implant [5]. Furthermore, frequency sensitivity of the auditory nerves along the cochlea is strongly dependent on spatial location as well as the relative health condition and amount of nerve fibers present. Therefore, after implant, it is necessary for a patient to go through a tuning procedure for speech processor optimization so that the cochlear implant can function properly [6]. In this tuning procedure, an audiologist will present different auditory stimuli consisting of basic sounds or words to a patient. The acoustic information will be detected by the implanted accelerometer and converted into an electrical signal. The speech processor will then process the signal and filter it into a group of outputs, which represent the acoustic information in an array corresponding to individual cochlear electrode bandwidth. Then, an array of biphasic current pulses with proper amplitude and duty cycle will be delivered to stimulate the electrodes located inside the cochlea along the auditory nerve. This excitation activates neurotransmitters, which travel to the brain for sound reception. The patient will then provide feedback in terms of speech reception quality to the audiologist. To achieve optimal performance for the active implant-human interface network, the audiologist will adaptively tune the speech processor through the RF-coils-based wireless link. Through the same link, an intelligent power management network for extending the battery longevity and ensuring patient safety can also be implemented between the implanted rechargeable battery and external powering electronics. An external coil loop worn in a headset can transmit RF power across the skin to the subcutaneous receiving loop, and active monitoring and control of incident RF power can be realized. Upon completion of battery charging, the communication and control unit can send out a wireless command to turn off the external powering system.

Attachment of the accelerometer at an ossicular location exhibiting the greatest vibration amplitude responding to an external acoustic stimulus will result in the most efficient sensing performance. Published data indicate that the umbo vibrates with the largest vibration amplitude in response to auditory inputs [7]–[9]. Measurements of ossicular bone vibration can be performed by using a laser Doppler vibrometer (LDV). Techniques employing LDV systems are well documented in both clinical and research environments [10], [11]. However, previously reported measurements have been performed along a direction perpendicular to the tympanic membrane. Due to the curved umbo surface, it is possible that the device may become misaligned anterior or posterior to the long process of the malleus during attachment, which could potentially degrade sensitivity. Therefore, it is necessary to investigate and characterize the umbo vibration response along different axes. In this research, the direction perpendicular to the tympanic membrane is defined as the primary axis of the umbo, and the vector parallel to the tympanic membrane plane and perpendicular to the long process of the malleus is defined as the secondary axis of the umbo, as depicted in Fig. 2 for illustration purpose. Measurement data obtained on umbo along the two axes can provide better understanding of sensor performance associated with any device position misalignment and can also be used as a design guideline for the MEMS accelerometer development.

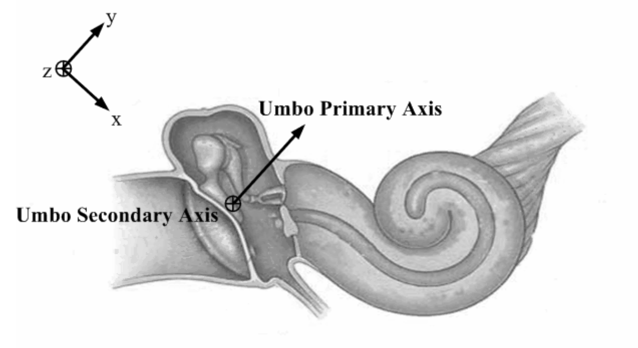


Fig. 2. Illustration of axes characterized by LDV. Relative to the axes shown in the inset, the umbo primary axis is along the y – axis, and the umbo secondary axis is measured along the z – axis into the plane of the picture.

Section II focuses on human temporal bone vibration characterization. Section III reports the measurement results of a commercial accelerometer attached on the umbo with conclusions and future work presented in Section IV.

## II. Human Temporal Bone Vibration Characterization

### A. Human Temporal Bone Preparation

Four cadaveric temporal bones were used to study the vibration characteristics of the umbo. The bones were kept stored in 1:10,000 merthiolate in 0.9% saline solution to maintain soft tissue compliance and hydration after thawing. All temporal bones were individually inspected under a microscope to verify an intact tympanic membrane, ear canal, and ossicular bone structure. Any bone with any evidence of pathology or structural damage due to middle ear cavity exposure was not used.

Temporal bones were then sequentially opened in two stages. A simple mastoidectomy with a facial recess approach was performed first. After the initial opening of the middle ear cavity, the temporal bone was further opened in a second stage of drilling. In this stage, the facial recess was widened such that full access was gained into the middle ear. The drilling proceeded until the tympanic membrane could be visualized. The bone was then thoroughly rinsed in saline and two pieces of 1 $mm^2$ reflective material, each weighing approximately 50 micrograms, were placed as targets for the umbo primary and secondary axes characterization.

### B. Temporal Bone Experimental Setup and Procedures

Fig. 3 depicts a schematic drawing of the temporal bone characterization setup. A temporal bone under examination was placed in a weighted temporal bone holder. An insert earphone driven by a waveform generator presented pure tones within the audible spectrum to the tympanic membrane. A probe microphone was positioned approximately 4 mm from the tympanic membrane to monitor the input sound pressure level. An LDV exhibiting a velocity resolution of 5 µm/s over the frequency range of DC to 50 kHz was used to measure the ossicles' vibrational characteristics. The laser was successively focused onto the reflective targets attached to the primary and secondary axes of the umbo.

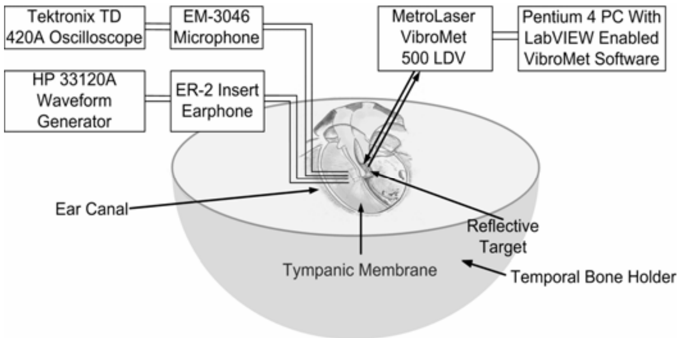


Fig. 3. Schematic of temporal bone setup.

The experimental equipment and a magnified view of the ossicles including measured points of interest are shown in Fig. 4. Fig. 4 (a) depicts the equipment and setup used in these measurements with a temporal bone secured in a temporal bone holder. Fig. 4 (b) magnifies the temporal bone and focuses on the area visible after a facial recess opening. The arrow points to a reflective target placed on the umbo for the secondary axis characterization. Fig. 4 (c) shows the temporal bone rotated 90 degrees after removing the medial wall of the middle ear. The arrow points to a reflective target placed on the umbo for characterizing vibration along the primary axis, which is the vibration in and out of the viewing plane. Acceleration of the umbo along the primary axis and the secondary axis was measured in the frequency range of 250 Hz to 10 kHz with input tones between 70 dB and 100 dB SPL in increments of 5 dB.

### *C. Measurement Results and Discussion*

Fig. 5 (a) compares the average peak-to-peak acceleration of the umbo measured along the primary axis and along the secondary axis in four cadaveric ears, stimulated by an input tone of 80 dB, 90 dB, and 100 dB SPL within the audible spectrum. The acceleration frequency response along the

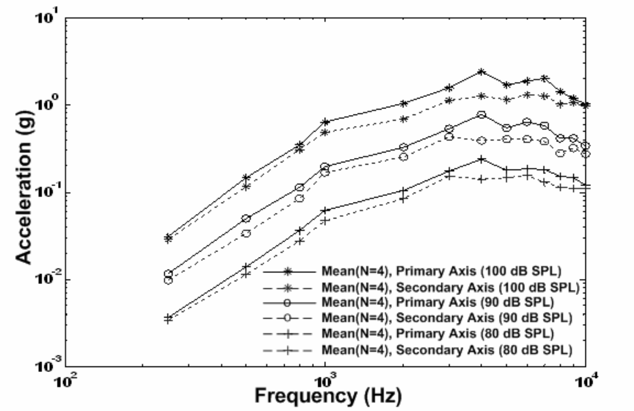


(a)

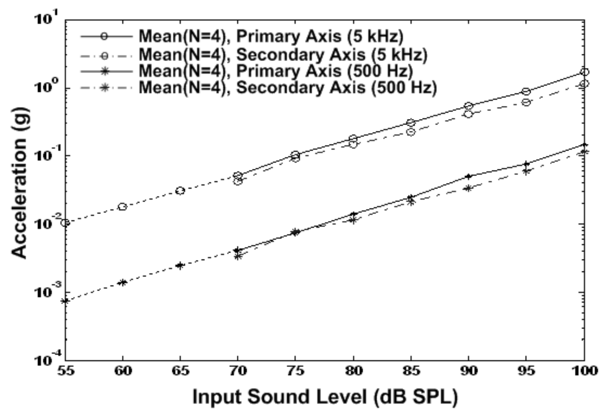


(b)

Fig. 5. Acceleration response curves. (a) Acceleration frequency response at 80 dB, 90 dB, and 100 dB SPL. (b) Loudness response at 500 Hz and 5 kHz. Dashed lines below 70 dB SPL represent the projected primary axis acceleration amplitude based on 20 dB per decade slope.

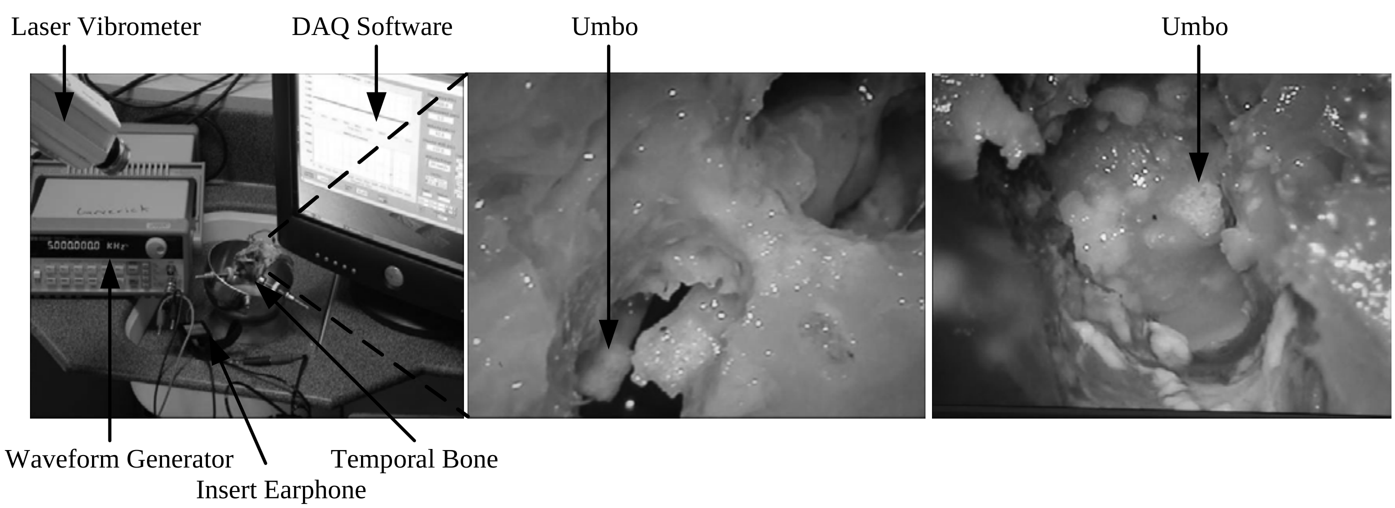


(a) (b) (c)

Fig. 4. (a) Photograph of equipment used in characterizing temporal bone vibrational response. (b) Magnified view of temporal bone focusing on the ossicles visible after facial recess opening. (c) View of temporal bone rotated 90 degrees after medial wall removal.

primary axis is nearly identical to that along the secondary axis. The acceleration amplitude increases with a slope of 40 dB per decade from 250 Hz to 1 kHz and with a slope of about 20 dB per decade from 1 kHz to 4 kHz. Above 4 kHz the acceleration signal remains relatively flat. Although the frequency trends are very similar, a 20% increase in acceleration amplitude is measured on the umbo along the primary axis compared to the secondary axis. While the difference between the two axes measurement is small, it occurs with approximately equal magnitude in all bones at all sound levels. Therefore, any potential misalignment in sensor placement will have a minimal impact on the output signal amplitude because of the similar acceleration amplitude response, and also negligible frequency distortion due to the similar frequency response. Fig. 5 (b) shows the corresponding average peak-to-peak acceleration of the umbo along the primary and secondary axes as a function of input sound level at 500 Hz and 5 kHz, indicating a linear relationship of 20 dB per decade over the range from 70 dB and 100 dB SPL at each frequency. As depicted in the figure, this allows for an acceleration projection for input sound level below 70 dB SPL, which is the resolution limit of the LDV measurement system.

These measurement results can serve as a design guideline to help define the specifications for the prototype accelerometer. Audiologists report that audible speech is primarily focused between 500 Hz and 8 kHz, and that the loudness of quiet conversation is approximately 55 dB SPL. From Fig. 5 (a) it can be seen that within the audible speech spectrum, 500 Hz has the lowest acceleration response, and thus it is the most difficult for detection. The projected amplitude along the primary axis at 500 Hz and 55 dB SPL in Fig. 5 (b) is approximately 700 µg. Today's state-of-the-art cochlear implants have multiple channels and electrodes to provide an appropriate stimulus to the correct location within the cochlea. At 500 Hz, the electrode channel bandwidth is on the order of 200 Hz. Therefore, to detect sounds at 55 dB SPL at 500 Hz, an accelerometer with a sensitivity of 50 $\mu g/\sqrt{Hz}$ and a bandwidth of 10 kHz is needed. From Fig. 5 (a) it can also be seen that within the audible spectrum the maximum acceleration amplitude is about 3 g.

Another important design consideration is the total device mass. The mass of the umbo and long process of the malleus is about 20 – 25 milligrams. It has been shown [12], [13] that adding a mass greater than 20 milligrams can potentially result in a significant damping effect on the frequency response of the middle ear ossicular chain, particularly at frequencies above 1 kHz. Therefore, the total mass of the packaged sensing system needs to be kept below 20 milligrams.

## III. Acoustic Vibration Measurement of Human Temporal Bone With A Commercial Accelerometer

A commercial accelerometer, an Analog Devices ADXL 320 shown in Fig. 6, was used to verify the concept of sensing bone vibration and converting the vibration to an electrical signal. The ADXL 320 was chosen because it has the smallest package size commercially available. The dimensions of the ADXL 320 are 4 mm x 4 mm x 1.45 mm, with a mass of 85 milligrams. The ADXL 320 exhibits a sensitivity of 123 $mV_{rms}/g$ with a noise floor of 250 $\mu g_{rms}/\sqrt{Hz}$ from a 3 volt supply. The device can measure a peak acceleration of 5 g. It also has a variable bandwidth up to 2.5 kHz. Although the bandwidth is smaller than desired, and the mass is larger than required, the ADXL 320 is sufficient to detect temporal bone vibration to verify the proposed concept.

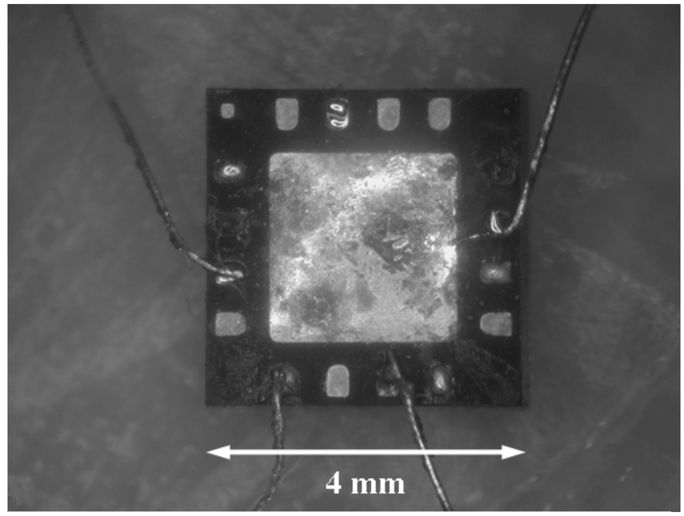


Fig. 6. Photograph of ADXL 320 used to detect temporal bone vibrations. Dimensions are 4 mm x 4 mm x 1.45 mm.

Another temporal bone was prepared as described in Section II A. An optical characterization with the LDV was performed on this bone along the primary umbo axis as described in Section II B before attaching the accelerometer. The results of the optical characterization at 80 dB SPL and 100 dB SPL are presented in Fig. 7, and are in good agreement with the average data obtained from the four temporal bones recorded earlier.

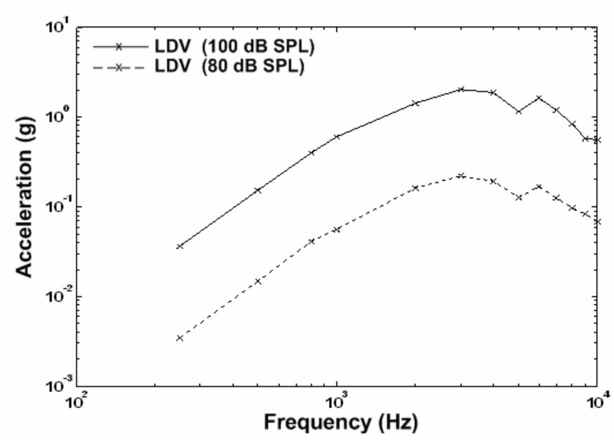


Fig. 7. Acceleration frequency response measured by the LDV along the umbo primary axis at 80 dB and 100 dB SPL.

A piece of double-sided adhesive was first placed on the back of the ADXL 320. After orienting the sensor in the direction of the primary axis at a few millimeters above the umbo, gentle pressure was applied for 30 seconds to attach the accelerometer to the temporal bone as shown in Fig. 8. The arrow represents the direction of motion along the primary axis. Input tones from 300 Hz to 2.4 kHz were presented to the tympanic membrane in decreasing increments of 5 dB starting at 100 dB SPL. Acceleration measured by the accelerometer was then recorded. The ADXL 320 was also used as a target for the LDV to simultaneously record acceleration optically to confirm measurement accuracy.

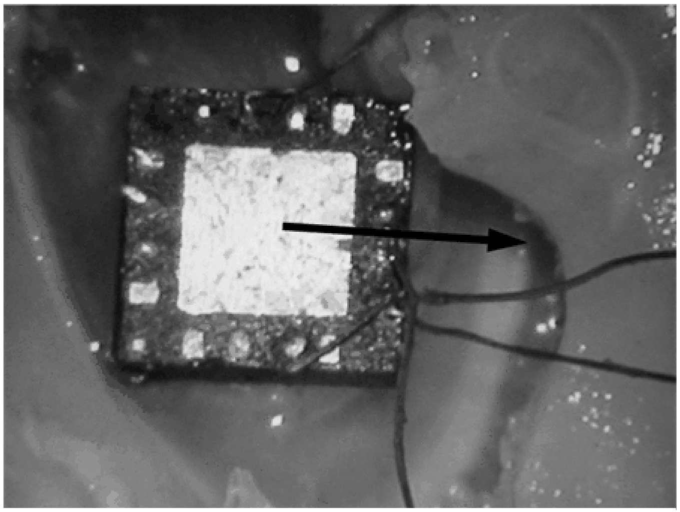

Fig. 8. Photograph of ADXL 320 attached to the umbo of a temporal bone. Arrow indicates direction of primary axis motion.

Fig. 9 reports the acceleration frequency response of the temporal bone measured electrically and optically with the accelerometer attached on umbo, and compares the data to the optical measurement characterization performed before the sensor attachment onto the umbo. As expected, the electrically measured acceleration frequency response with the accelerometer attached on the umbo is virtually identical to the optical measurements taken with the LDV. However, compared to the LDV measurement without the sensor attachment, there is approximately a 10 – 15 dB suppression of amplitude. This is due to the relatively heavy mass of the accelerometer, which loads the ossicles and damps the response.

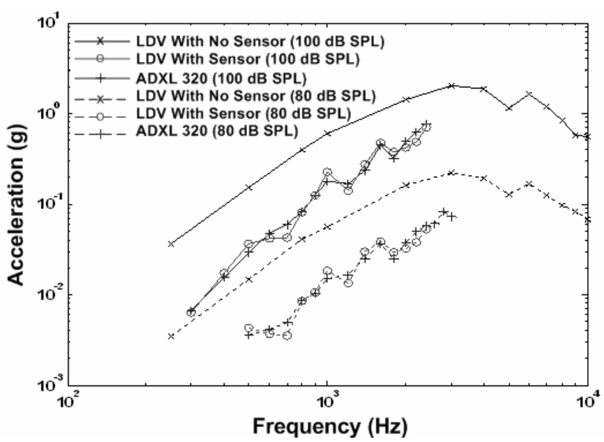


Fig. 9. Acceleration frequency response measured along the umbo primary axis at 80 dB and 100 dB SPL.

Fig. 10 shows the noise floor of the ADXL 320 measured by a dynamic signal analyzer with a resolution bandwidth of 61 Hz. The noise floor amplitude of 29 $\mu V_{rms}/\sqrt{Hz}$ is equivalent to a minimum detectable acceleration amplitude of about 2 mg. Fig. 11 displays the acceleration measurement plot with a resolution bandwidth of 61 Hz, corresponding to an input stimulus of 100 dB SPL at 2.4 kHz. The displayed signal to noise ratio is approximately 52 dB, which is equivalent to a detection of a 55 dB SPL sound at the same frequency with a bandwidth of 200 Hz. Fig. 12 presents the acceleration versus input sound level responses measured by the ADXL 320 along the primary axis at 500 Hz and 2.4 kHz for a resolution bandwidth of 61 Hz. The solid line at 2 mg represents the accelerometer noise floor. Extrapolating the measurement data indicates that minimum input sound levels of approximately 80 dB SPL at 500 Hz and 55 dB SPL and 2.4 kHz can be detected by the sensor. A further miniaturized system with improved sensitivity is, therefore, needed to detect normal conversation levels.

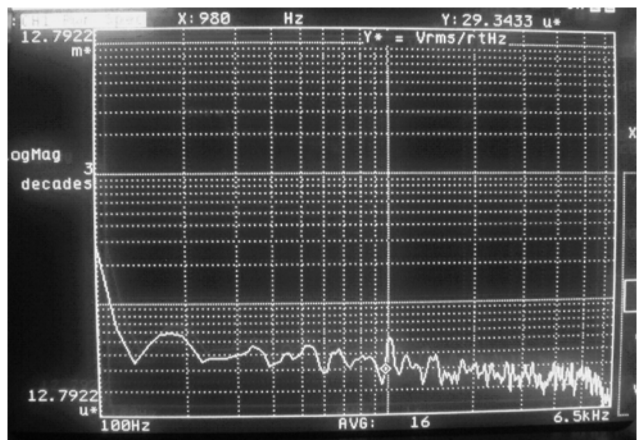


Fig. 10. Frequency spectrum showing the noise floor of the ADXL 320 while on temporal bone.

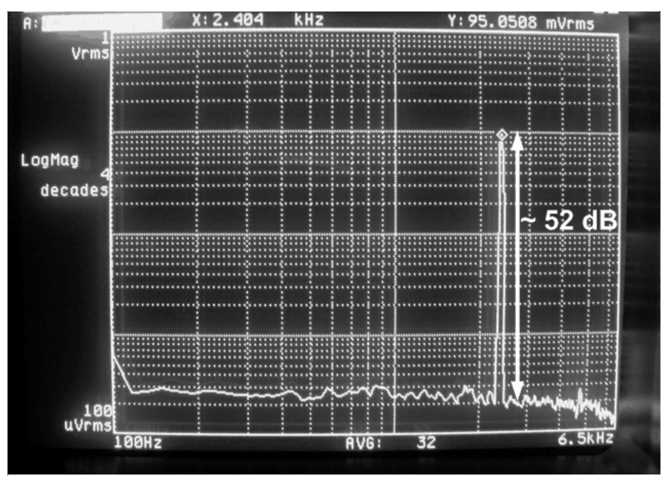


Fig. 11. Frequency spectrum showing a 2.4 kHz tone at 100 dB SPL measured by the ADXL 320. Signal to noise ratio is approximately 52 dB at this frequency.

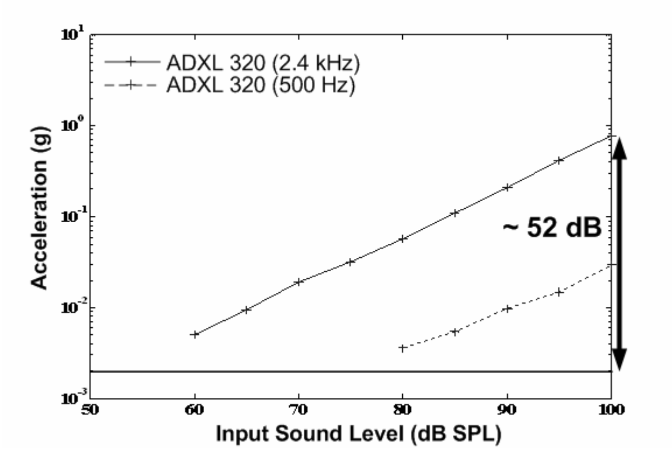


Fig. 12. Acceleration versus input sound level responses measured by the ADXL 320 along the primary axis at 500 Hz and 2.4 kHz. Solid line at 2 mg represents the accelerometer noise floor.

## IV. CONCLUSION

Characterization of the temporal bone to determine the effect of potential misalignment of an implantable MEMS sound sensor has been reported. The feasibility of attaching an accelerometer to the middle ear ossicular chain to detect an acoustic stimulus has been demonstrated. A sensor exhibiting a total package mass below 20 milligrams and a sensitivity of 50 $\mu g/\sqrt{Hz}$ is required in order to sense and reconstruct normal conversation. However, the ADXL 320 has demonstrated the viability of the prototype system concept of utilizing an accelerometer attached on the umbo as a means of transducing sound-induced vibration into an electrical signal for future totally implantable cochlear prosthetic systems. A fully integrated MEMS accelerometer achieving the aforementioned requirements is currently under development.

## REFERENCES

[1] H. P. Zenner, J. W. Baumann, G. Reischl, *et. al.*, "Patient selection for incus body coupling of a totally implantable middle ear implant," *Acta Otolaryngology*, vol. 123(6), pp. 683-696, August 2003.

[2] G. R. Ball, A. Huber, and R. L. Goode, "Scanning laser Doppler vibrometry of the middle ear ossicles," *Ear, Noise, and Throat Journal*, vol. 76, pp. 213-218, 220, 222, 1997.

[3] K. J. Dormer and R. Z. Gan, "Biomaterials for implantable middle ear hearing devices," *Otolaryngology Clinics of North America*, vol. 34, pp. 289-297, 2003.

[4] W. H. Ko, W. L. Zhu, M. Kane, and A. Maniglia, "Engineering principles applied to implantable otologic devices." *Otolaryngology Clinics of North America*, vol. 34, pp. 299-314, 2001.

[5] T. E. Bell, K. D. Wise, D. J. Anderson, "A Flexible Micromachined Electrode Array for a Cochlear Prosthesis," *Transducers 1997*, pp. 1315-1318, Chicago, June 16-19, 1997.

[6] P. C. Loizou, "Mimicking the Human Ear: An Overview of Signal-Processing Strategies for Converting Sound into Electrical Signals in Cochlear Implants," *IEEE Signal Processing Magazine*, pp. 101-130, September 1998.

[7] S. E. Voss, J. J. Rosowski, S. N. Merchant, and W. T. Peake, "Acoustic responses of the human middle ear," *Hearing Research*, vol. 150, pp. 43-69, 2000.

[8] J. J. Rosowski, P. J. Davis, S. N. Merchant, K. M. Donahue, and M. D. Coltrera, "Cadaver middle ears as models for living ears: comparisons of middle ear input impedance," *Annals of Otology, Rhinology, and Laryngology*, vol. 99, pp. 403-412, 1990.

[9] R. Z. Gan, M. W. Wood, and K. J. Dormer, "Human middle ear transfer function measured by double laser interferometry system," *Otology & Neurotology*, vol. 25, pp. 423-435, 2004.

[10] K. R. Whittemore Jr., S. N. Merchant, B. B. Poon, and J. J. Rosowski, "A normative study of tympanic membrane motion in humans using a laser Doppler vibrometer," *Hearing Research*, vol. 187, pp. 85-104, 2004.

[11] R. L. Goode, G. Ball, and S. Nishihara, "Measurement of umbo vibration in human subjects – method and possible clinical applications," *American Journal of Otology*, vol. 14, pp. 247-251, 1993.

[12] S. Nishihara, H. Aritomo, and R. L. Goode, "Effect of changes in mass on middle ear function," *Otolaryngology Head and Neck Surgery*, vol. 109, pp. 899-910, 1993.

[13] R. Z. Gan, M. W. Wood, R. K. Dyer, and K. J. Dormer, "Mass loading on the ossicles and middle ear function," *The Annals of Otology, Rhinology and Laryngology*, vol. 110, pp. 478 – 485, May 2001.